Role of Static Displacements in Stabilizing Body Centered Cubic High Entropy Alloys

G. D. Samolyuk, Y. N. Osetsky, G. M. Stocks, and J. R. Morris

Title: The role of static displacements in stabilizing body centered cubic high entropy alloys

Authors: G. D. Samolyuk*[1], Y. N. Osetsky[1], G. M. Stocks[1], J. R. Morris**[2]

Affiliations:

[1]Materials Science and Technology Division, Oak Ridge National Laboratory, Oak Ridge, TN 37831, USA

[2]Ames Laboratory, Iowa State University, Ames, IA 50011

*Correspondence to: * samolyukgd@ornl.gov, ** morrisj@ameslab.gov

Abstract

The configurational entropy of high entropy alloys (HEAs) plays little role in the stabilization of one *particular* crystal structure over another. We show that disorder-induced atomic displacements help stabilize body-centered cubic (bcc) structure HEAs with average valences <4.7. These disorder-induced atomic displacements mimic the temperature-induced vibrations that stabilize the bcc structure of group IV elemental metals at high temperatures. The static displacements are significantly larger than for face-centered cubic (fcc) HEAs, approaching values associated with the Lindemann criterion for melting.

One Sentence Summary: Chemical disorder in high entropy alloys have a previously unidentified, *non-entropic* energy contribution that stabilizes a particular crystalline ground state.

High entropy alloys (HEAs), single-phase solid-solutions alloys comprised of 4 or more components at or near equiatomic concentration, frequently crystallize as chemically disordered solid-solutions with face-centered cubic (fcc) [1,2], body-centered cubic (bcc) [3], and hexagonal close-packed (hcp) [4-8] crystal structures. HEAs exhibit a number of very interesting electronic transport [9] and mechanical properties [10-14]. The simplest explanation of the existence of the disordered phase is the large entropy of mixing associated with the high concentrations of all species. Much less is known regarding the mechanisms that determine the *specific* crystal structure selected, i.e. fcc, bcc, or hcp. Understanding the competing crystal structures is important for essentially all properties. As a particular example, transformation-induced plasticity (TRIP) may improve their ductility of bcc HEAs, by allowing for deformation-induced transitions [14-17]. Such transformations have been observed in bcc HEAs formed of group IV and V metals [14,17], and are sensitive to the energy associated with the transformations between the relevant phases.

For elemental $4d$, $5d$ transition metals, there is a well-known connection between ground state structure and d band filling [18], where the ground state structure of the elemental $4d$, $5d$ transition metal series follow the sequence hcp – bcc – hcp – fcc while moving from empty to completely filled d-electron shells. Often, low-temperature close-packed structures transform to the more "open" bcc structure at higher temperatures, driven by the vibrational entropy associated with low-lying phonon modes of the bcc phase [19-22], particularly those associated with the T1 branch in the $[0\zeta\zeta]$ direction, and the corresponding $C' = $ ½ $(C_{11} - C_{12})$ elastic constant. For group IV metals, first-principles calculations have shown that at $T = 0$, C' is negative for the bcc phase, indicating a mechanical instability [23,24] at low temperatures. The anharmonicities associated with these modes, and their coupling to other modes, leads to stabilization at higher temperatures [25,26]. Accordingly, these modes are stable but finite in the high-temperature bcc phase [19-22]. Alloys

containing group IV metals (hcp) may exhibit interesting related mechanical properties, such as the Ti-Nb "gum metal" [27] or the shape memory effect in NiTi [28-31].

We examine the trend associated with *d*-band filling for bcc HEAs formed from various combinations of group IV and V transition metal elements, using composition to vary the average number of valence electrons, ranging from 4 to 5. We demonstrate that chemical disorder gives rise to a new energetic contribution that significantly affects the competition between crystal structures, in some cases changing the ground-state structure. Specifically, we have performed density-functional theory [32] (DFT) calculations of a series of HEAs with varying *<Z>*, to examine the effects of disorder on the energetics, phonon properties, and phase stability. The calculations show that static random lattice distortions in these alloys can stabilize the bcc structure. This energetic stabilization

Fig 1. bcc phonon dispersion calculated in a) Zr; b) HfNbZrTi, and c) VNbTa solid solutions, with atoms occupying the perfect bcc lattice sites. Negative frequencies with minima at N- and L-points of the Brillouin zone manifest structural instabilities structures. The similarity of (a) and (b) underlines the similar dynamical instabilities for these cases, in contrast with (c).
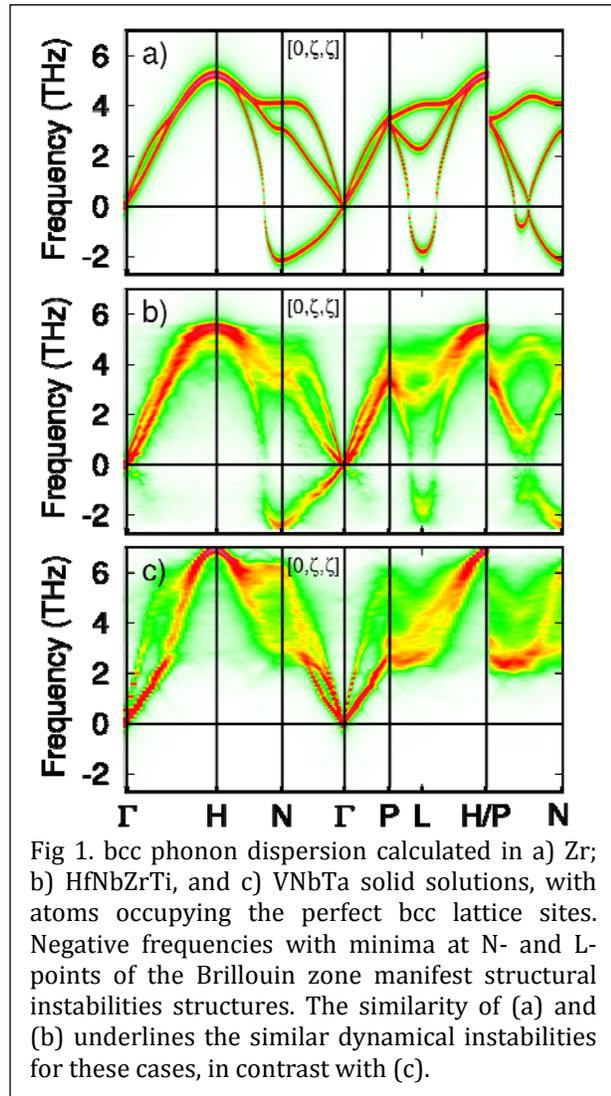
of certain bcc HEAs is a novel manifestation of the disorder in these materials, and provides new insight into the role of disorder in determining the phase behavior of these alloys.

Chemical disorder in the alloys was simulated using special-quasirandom-structure (SQS) [33] models (See Supplemental Materials) in supercells containing 54 atoms

for phonon calculations and 256 atoms to calculate the energy surface of the Burgers transformation. The details of the VASP calculations [34], including the use of the UPHO [https://github.com/yuzie007/upho] and PHONOPY packages [35] for phonon calculations, are given in the Supplemental Information, section S2, including references to [36-38].

Figure 1 compares the calculated phonon dispersion of two bcc alloys, HfNbZrTi and VNbTa, as well as elemental bcc Zr. These were calculated with atoms at ideal bcc lattice positions using supercell phonon unfolding (SPU) simulations based on large supercell models of the disordered state [39-42]. The calculated phonons for VNbTa (formed entirely of Group V elements) are all stable; those for HfNbZrTi, however, show a strong lattice instability, with the T1 [110] branch being entirely imaginary (shown as negative frequencies) with a minima at the N-point and near the L-point. These instabilities are normally associated with transitions to the hcp and ω phases, respectively. Notably, these same unstable phonons are also observed in bcc Zr (Fig, 1a), where again the lowest minimum at the N-point phonon is associated with the transformation pathway to the hcp phase discussed below.

To check the sensitivity of the phonons to the particular chemical arrangement in the supercell, the phonon dispersion of HfNbZrTi was calculated in several SQS structures, two with (different) ideal random arrangements of atoms and one with significant chemical sort-range-order (SRO) (See Supplemental Materials S2 and S3). As is evident from Fig. S2 and S3, the calculated phonon dispersions (spectral functions) of the two ideal random SQS's are essentially identical, as is the overall structure of short-range-ordered SQS. This insensitivity of the phonon dispersion relations to the fine details of the atomic arrangement is a direct consequence of the large degree of disorder smearing, in energy and wave-vector, that results from the large atomic mass differences (factors of ~2) between the various 3d-, 4d- and 5d-transition-metal alloying elements. The addition of the force-constant randomness that is also endemic to the disordered state only further increases the phonon broadening [43]. Disorder smearing of the spectral function that is a substantial

fraction of a Brillouin dimension implies a phonon mean-free-path that is the order of a few interatomic spacings, a situation well captured using SQS based methods. The clear systematic trends of phonons with <Z> (Supplemental Fig. S5) is also indicative that the phonon dispersions are not highly sensitive to the particular arrangement of atoms within the computational cell whilst allowing the capture of phonon instabilities.

Both alloys shown in Fig. 1 are known to be stable in the bcc phase [44] (and potentially at lower temperatures as well). Given that the HfNbZrTi system shows calculated phonons similar to Zr, why then is bcc HfNbZrTi observed at low temperatures, whereas bcc Ti, Zr, and Hf are only stable above ~1000 K? We demonstrate that large, environment-dependent atomic displacements in HfNbZrTi, resulting from underlying chemical disorder, energetically stabilize the bcc phase even at T=0.

Figure 2 examines the bcc→hcp structural transition pathway, conventionally described in terms of the Burgers path [45-47]. The Burgers path (Figure 2b) is an energy surface corresponding to two degrees of freedom: First, a tetragonal strain, λ, distorts atomic positions into a equilateral triangular lattice [47]. Second, lateral shifts of alternating [110] planes in the [$1\bar{1}0$] direction (associated with the N-point T_1 phonon [48]) complete the transformation. In Fig. 2c-g, the point (0,0) in the (λ, ξ) plane corresponds to the bcc structure, and (λ, ξ) =(1,1) corresponds to hcp. The $\lambda = 0$ energy cross section of Figs. 2c and 2e, for Zr [48] and HfNbZrTi, shows that the frozen phonon energy [23,48], as function of phonon amplitude ξ, displays a negative second derivative (without relaxations for HfNbZrTi), defining a negative N-point T_1 phonon frequency – consistent with Fig. 1. Both bcc Zr and HfNbZrTi have a similar behavior near $\lambda = 0$, indicating that, the bcc phase is unstable. The minima for Zr and HfNbZrTi are different: the global minimum in the (λ, ξ) plane is located at (1, 1) in Zr (Fig. 2e), i.e, the hcp structure, while in HfNbZrTi it is located close to (0.02, 0.47) – essentially, having a small value of λ, formed by a *static* amplitude of the NT$_1$ phonon. This is similar to results reported for TiV and HfTa

[46]. In the following we refer to structures of this type as body centered tetragonal (bct) with hcp modulation.
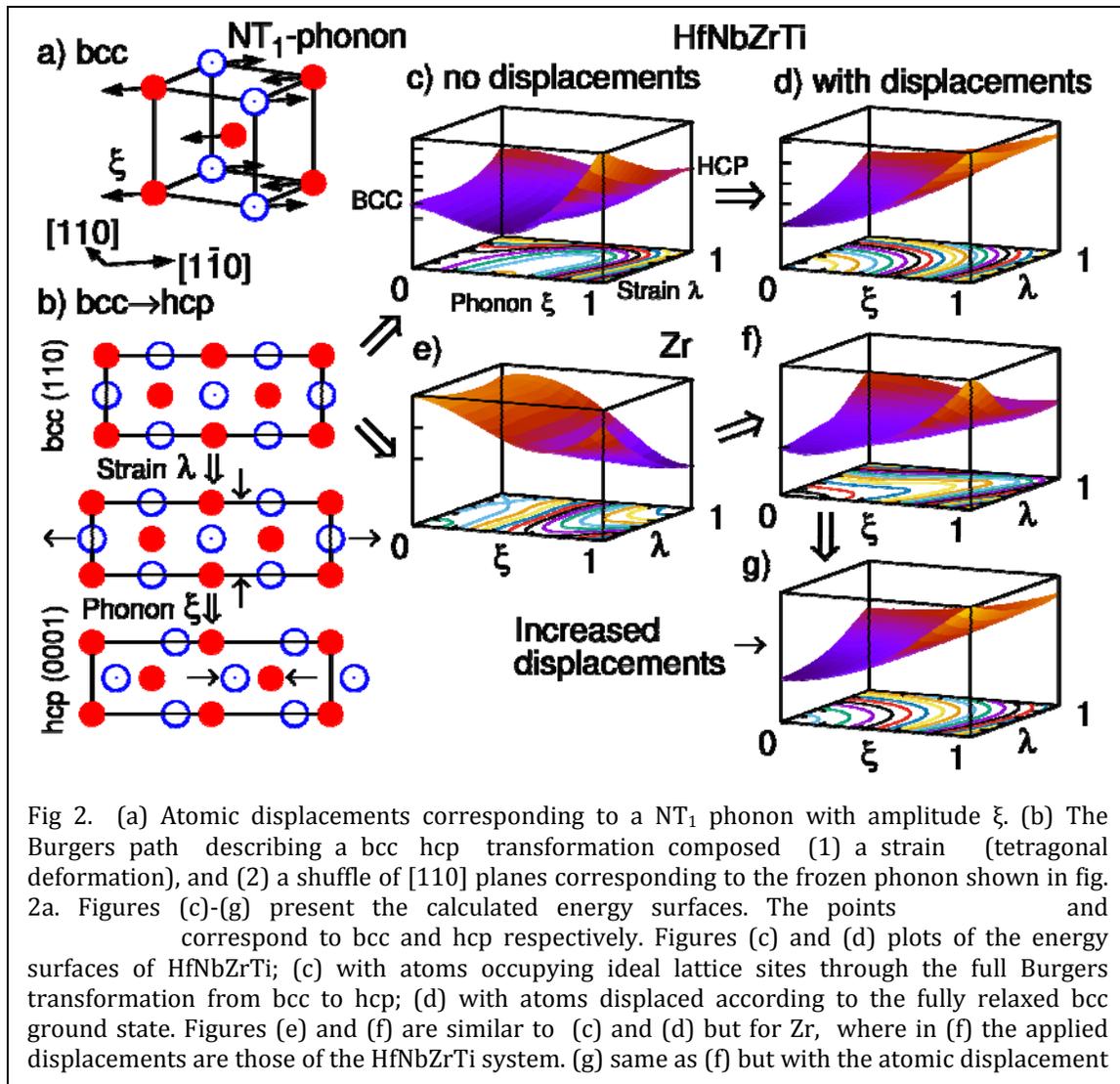
Fig 2. (a) Atomic displacements corresponding to a NT_1 phonon with amplitude ξ. (b) The Burgers path describing a bcc hcp transformation composed (1) a strain (tetragonal deformation), and (2) a shuffle of [110] planes corresponding to the frozen phonon shown in fig. 2a. Figures (c)-(g) present the calculated energy surfaces. The points   and   correspond to bcc and hcp respectively. Figures (c) and (d) plots of the energy surfaces of HfNbZrTi; (c) with atoms occupying ideal lattice sites through the full Burgers transformation from bcc to hcp; (d) with atoms displaced according to the fully relaxed bcc ground state. Figures (e) and (f) are similar to (c) and (d) but for Zr, where in (f) the applied displacements are those of the HfNbZrTi system. (g) same as (f) but with the atomic displacement

The magnitude of the static displacements depend upon d-band filling, and can be large. Results for the root mean square displacement per atom,   ‾, are shown in Fig. 3 for a series of alloys (Supplementary materials Table S1). The largest value is Δ=0.3 Å, or 9% of the bcc lattice parameter, for HfNbZrTi. This reduces to   as <Z> goes from 4.25 to 5. The values for <Z> greater than 5 are even

smaller than that of VNbTa, despite having more constituents and therefore more local configurations. In Fig. 3, we also show the range of (0.04-0.75 Å) for a variety of fcc-based solid solutions, obtained from theoretical calculations [49,50] and diffraction experiments [51]. All bcc alloys have significantly larger displacements (see also

Fig 3. Calculated rms displacement ____ ,in a series of high entropy bcc alloys, where is the average number of valence electrons. The yellow bar indicates the range of values expected for fcc HEAs (shown independent of).
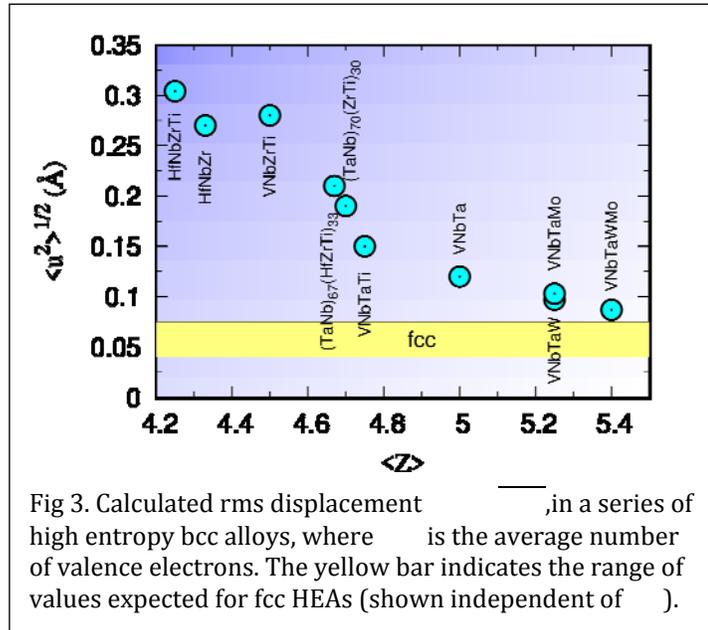
[52]), particularly for lower values of <Z>. Recent theoretical [53,54] and experimental [55] work also note the large displacements with increasing Ti, Zr, Hf concentration.

The large anharmonic phonon coupling produced by temperature-induced atomic vibration was used to explain high temperature stabilization of bcc Zr [24,26]. For HfNbZrTi, the calculations above show that T=0 displacements similarly appear to stabilize the bcc phase. To check this, we calculated phonons for pure Zr using the HfNbZrTi relaxed structure (i.e., a bcc lattice with local distortions corresponding to those in HfNbZrTi). For Zr, the value of from HfNbZrTi corresponds to thermal atomic vibrations at 1200 K, estimated using the Debye model (Supplementary materials Fig. S4). This temperature is slightly higher than the experimental bcc→hcp transition temperature for Zr, 1135 K. The resulting Burgers path surface for this distorted structure (Fig. 2f) differs significantly from the ideal case (Fig. 2e). The hcp phase energy now corresponds to a local maximum (Fig. 2f) and the transition to the hcp structure is suppressed. The minimum energy is very close to the (0, 0) point corresponding to the bcc structure. A calculation based on a further increase of atomic displacements by 50% completely stabilizes

the Zr bcc structure (Fig. 2g). This is further supported by calculations of Zr bcc structures with the distorted structure (see supplemental section S1, particularly fig. S1). (Section S1 also notes other approaches for calculating effective phonons at high temperatures, particularly those in Refs. [56,57]). We expect larger displacements in the bcc phase at T=1200 K than the simple estimate here, due to an expected lower Debye frequency for the bcc phase than that for hcp.

Relaxed displacements in HfNbZrTi not only alter the transformation path energy surface but also stabilize the phonons, particularly the T1 branch in the direction, as well as those near the L point at 2/3 [ζ ζ ζ] (Fig. 4). The phonon dispersion at small
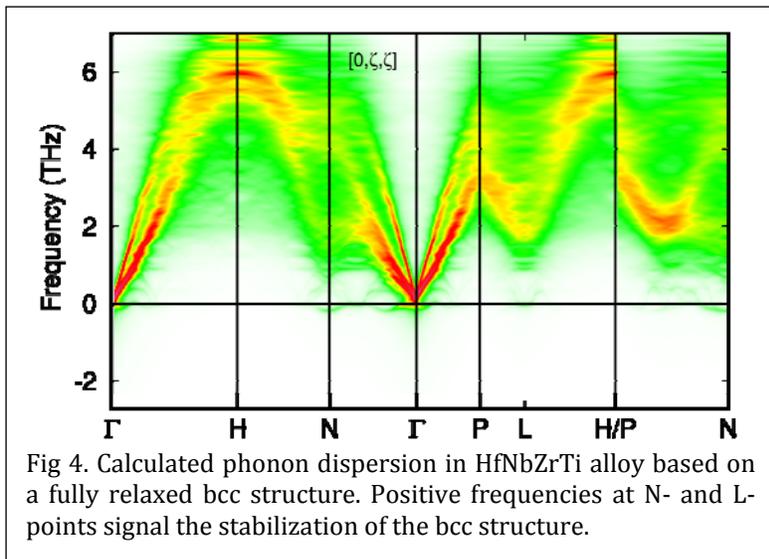
Fig 4. Calculated phonon dispersion in HfNbZrTi alloy based on a fully relaxed bcc structure. Positive frequencies at N- and L-points signal the stabilization of the bcc structure.

results in a small, positive modulus [58,59]. This phonon dispersion is based on an SQS structure; supplemental Figure S2 compares this with a Monte-Carlo relaxed structure found using the approach of [60] and based on the enthalpy matrix described in [61], finding very similar results.

Supplementary materials S5, Fig. S5 show the phonon dispersion dependence on *d*-band filling in a series of HEAs, with ranging from 4-5: HfNbZrTi, HfNbZr, VNbZrTi, $(TaNb)_{67}(HfZrTi)_{33}$, $(VTaNb)_{67}(HfZrTi)_{33}$, $(TaNb)_{70}(ZrTi)_{30}$, VNbTaTi, VNbTa. In the limiting case of VNbTa with , the relatively small lattice relaxation (Å) doesn't significantly change the phonon dispersion from that shown in Fig. 1c. Increasing results in fewer negative modes and eventually stabilizes the branch. In all cases considered, relaxing the bcc structure stabilizes essentially all phonon modes.

The hcp phase becomes more stable, as the effective valence goes from 5 to 4.25. This is reflected in the energy difference E_{hcp}-E_{bcc} between hcp and bcc solid solutions decreasing as $\langle Z \rangle$ decreases. For relaxed configurations, this difference changes from 352 meV/atom in VNbTa (Fig. S6) to 141 meV/atom in HfNbZrTi. The atomic positions in the hcp structure are a result of the Burgers transformation of the bcc relaxed structure; further relaxation of the hcp lattice with a constrained *c/a* ratio reduces the difference to 35 meV/atom in HfNbZrTi. (In VNbTa, the hcp structure is mechanically unstable, Fig S6) Further relaxation of atomic positions of HfNbZrTi from the energy minimizing configuration (Fig. 2c) located close to (0.02,0.47), results in the disappearance of the hcp modulation, and the structure converges very close to (0,0) (the ideal bcc structure).

The large displacements and soft phonons in these alloys provide an interesting contrast to classic theories of melting. In the Lindemann criterion [62], melting is expected when the mean square displacement, normalized to the near neighbor constant, reaches a value typically reported in the range of 0.07-0.12 [62-65]. The Born criterion [66] suggests that melting occurs close to the temperature at which one would expect an elastic constant to fully soften. For HfNbTiZr, the ideal BCC phase shows an elastic instability (similar to the Born criterion) at T=0 K, and with relaxations have a mean square displacement ~0.1 of the average nearest neighbor distance at 0K, satisfying the Lindemann criterion melting. Given these considerations, bcc HfNbTiZr would be expected to be close to melting by both the Lindemann and Born criteria, even at T=0 K! In contrast, these effects are closely coupled in this system, and actually stabilize the bcc phase: the large displacements stabilize the elastic mode and the bcc phase, all at T=0K.

In conclusion, first principles calculations of show that lattice distortions in group IV (Ti, Zr, Hf) and V (V, Nb, Ta) HEAs play an important, previously undescribed, role in stabilizing the bcc phase. These relaxations occur due to the configurational disorder; thus, the configurational disorder provides an *energetic* stabilization of the

bcc phase, in addition to any entropic contributions. For HEAs with $<Z> < 4.7$, the ideal bcc structure is mechanically unstable, but static distortions stabilize the phonons. This is similar to the temperature-driven stabilization of bcc Zr, where temperature-driven distortions stabilize the bcc structure. This stabilization effect is purely energetic, mimicking vibrational stabilization of the bcc phase even at 0 K.

These results are relevant to other effects, including vacancy diffusion and ductility in bcc HEAs. In alloys with $\langle Z \rangle < 4.7$, low frequency modes (precursors of structural transitions [67,68]) may significantly affect defect diffusion. For example, the vacancy migration energy in the bcc phase decreases dramatically close to the bcc-to-hcp transition in Zr [69]. In the bcc HEAs, the close competition between the bcc and hcp phases for $\langle Z \rangle < 4.7$ may have a similar effect as in Zr, leading to a significant reduction of diffusivity, i.e. sluggish diffusion. This diffusion suppression is expected to be amplified by disorder [70]. Finally, the significant reduction of the energy difference E_{hcp}-E_{bcc} as the valence $<Z>$ goes from 5 towards 4 may be a reason for significantly improved ductility observed in HfNbZrTiTa [10,12], where the formation of secondary phases under stress provides additional mechanisms for strain accumulation, i.e. transformation-induced plasticity (TRIP) [14-17]. Ultimately, the work here suggests that tuning composition to control $\langle Z \rangle$ provides a potential approach for controlling transformations in these materials, leading to potential enhancements in ductility through the TRIP mechanism, as well as control over diffusion kinetics.

Author Contributions: GDS, JRM, GMS, and YNO designed the research and performed theoretical calculations. GDS and JRM drafted the manuscript and all the other authors participated in further writing and discussions.

Competing interests: Authors declare no competing interests.

References
[1]   J. W. Yeh, S. K. Chen, S. J. Lin, J. Y. Gan, T. S. Chin, T. T. Shun, C. H. Tsau, and S. Y. Chang, Advanced Engineering Materials **6**, 299 (2004).
[2]   B. Cantor, I. T. H. Chang, P. Knight, and A. J. B. Vincent, Mat. Sci. Eng. A **375**, 213 (2004).
[3]   O. N. Senkov, G. B. Wilks, D. B. Miracle, C. P. Chuang, and P. K. Liaw, Intermetallics **18**, 1758 (2010).
[4]   J. Qiao, M. Bao, Y. Zhao, H. Yang, Y. Wu, Y. Zhang, J. Hawk, and M. Gao, Journal of Applied Physics **124**, 195101 (2018).
[5]   R. Soler, A. Evirgen, M. Yao, C. Kirchlechner, F. Stein, M. Feuerbacher, D. Raabe, and G. Dehm, Acta Materialia **156**, 86 (2018).
[6]   Y. Zhao, J. Qiao, S. Ma, M. Gao, H. Yang, M. Chen, and Y. Zhang, Materials & Design **96**, 10 (2016).
[7]   M. Feuerbacher, M. Heidelmann, and C. Thomas, Materials Research Letters **3**, 1 (2015).
[8]   A. Takeuchi, K. Amiya, T. Wada, K. Yubuta, and W. Zhang, Jom **66**, 1984 (2014).
[9]   K. Jin, B. C. Sales, G. M. Stocks, G. D. Samolyuk, M. Daene, W. J. Weber, Y. Zhang, and H. Bei, Scientific Reports **6**, 20159 (2016).
[10]   O. N. Senkov, J. M. Scott, S. V. Senkova, F. Meisenkothen, D. B. Miracle, and C. F. Woodward, J. Mater. Sci. **47**, 4062 (2012).
[11]   F. Otto, A. Dlouhy, C. Somsen, H. Bei, G. Eggeler, and E. P. George, Acta Mater. **61**, 5743 (2013).
[12]   E. P. George, D. Raabe, and R. O. Ritchie, Nature Reviews Materials (2019).
[13]   C. Varvenne, A. Luque, and W. A. Curtin, Acta Mater. **118**, 164 (2016).
[14]   L. Lilensten, J.-P. Couzinié, J. Bourgon, L. Perrière, G. Dirras, F. Prima, and I. Guillot, Materials Research Letters **5**, 110 (2017).
[15]   Z. Li, K. G. Pradeep, Y. Deng, D. Raabe, and C. C. Tasan, Nature **534**, 227 (2016).
[16]   Z. Li, F. Körmann, B. Grabowski, J. Neugebauer, and D. Raabe, Acta Materialia **136**, 262 (2017).
[17]   H. Huang, Y. Wu, J. He, H. Wang, X. Liu, K. An, W. Wu, and Z. Lu, Advanced Materials **29**, 1701678 (2017).
[18]   D. G. Pettifor, Journal of Physics C: Solid State Physics **3**, 367 (1970).
[19]   C. Stassis and J. Zarestky, Solid state communications **52**, 9 (1984).
[20]   A. Heiming, W. Petry, J. Trampenau, M. Alba, C. Herzig, H. Schober, and G. Vogl, Physical Review B **43**, 10948 (1991).
[21]   W. Petry, A. Heiming, J. Trampenau, M. Alba, C. Herzig, H. Schober, and G. Vogl, Physical Review B **43**, 10933 (1991).
[22]   J. Trampenau, A. Heiming, W. Petry, M. Alba, C. Herzig, W. Miekeley, and H. Schober, Physical Review B **43**, 10963 (1991).
[23]   K.-M. Ho, C. Fu, and B. Harmon, Phys. Rev. B **29**, 1575 (1984).
[24]   Y.-Y. Ye, Y. Chen, K.-M. Ho, B. Harmon, and P.-A. Lindgrd, Physical review letters **58**, 1769 (1987).

[25]   Y. Y. Ye, Y. Chen, K. M. Ho, B. N. Harmon, and P. A. Lindgard, Phys. Rev. Lett. **58**, 1769 (1987).

[26]   P. Souvatzis, O. Eriksson, M. I. Katsnelson, and S. P. Rudin, Phys. Rev. Lett. **100**, 095901 (2008).

[27]   T. Saito *et al.*, Science **300**, 464 (2003).

[28]   Y. Y. Ye, C. T. Chan, and K. M. Ho, Phys. Rev. B **56**, 3678 (1997).

[29]   X. Huang, G. J. Ackland, and K. M. Rabe, Nat. Mater. **2**, 307 (2003).

[30]   S. Kibey, H. Sehitoglu, and D. D. Johnson, Acta Mater. **57**, 1624 (2009).

[31]   M. Krcmar and J. R. Morris, Journal of Physics: Condensed Matter **26**, 135401 (2014).

[32]   W. Kohn and L. J. Sham, Phys. Rev. **140**, 1133 (1965).

[33]   A. Zunger, S. H. Wei, L. G. Ferreira, and J. E. Bernard, Phys. Rev. Lett. **65**, 353 (1990).

[34]   Vienna Ab initio Simulation Package, http://cms.mpi.univie.ac.at/vasp/.

[35]   A. Togo and I. Tanaka, Scr. Mater. **108**, 1 (2015).

[36]   J. P. Perdew, K. Burke, and M. Ernzerhof, Phys. Rev. Lett. **77**, 3865 (1996).

[37]   P. E. Blöchl, Phys. Rev. B **50**, 17953 (1994).

[38]   G. Kresse and J. Furthmüller, Phys. Rev. B **54**, 11169 (1996).

[39]   T. B. Boykin, N. Kharche, G. Klimeck, and M. Korkusinski, Journal of Physics: Condensed Matter **19**, 036203 (2007).

[40]   T. B. Boykin, A. Ajoy, H. Ilatikhameneh, M. Povolotskyi, and G. Klimeck, Phys. Rev. B **90**, 205214 (2014).

[41]   Y. Ikeda, A. Carreras, A. Seko, A. Togo, and I. Tanaka, Phys. Rev. B **95**, 024305 (2017).

[42]   P. B. Allen, T. Berlijn, D. A. Casavant, and J. M. Soler, Phys. Rev. B **87**, 085322 (2013).

[43]   S. Mu *et al.*, (Mater, 2020).

[44]   A. S. Ahmad *et al.*, Journal of Applied Physics **121**, 235901 (2017).

[45]   W. G. Burgers, Physica **1**, 561 (1934).

[46]   B. Feng and M. Widom, Physical Review B **98**, 174108 (2018).

[47]   K. Masuda-Jindo, S. R. Nishitani, and V. Van Hung, Physical Review B **70**, 184122 (2004).

[48]   Y. Chen, C.-L. Fu, K.-M. Ho, and B. Harmon, Phys. Rev. B **31**, 6775 (1985).

[49]   N. L. Okamoto, K. Yuge, K. Tanaka, H. Inui, and E. P. George, **6**, 125008 (2016).

[50]   S. Mu, G. D. Samolyuk, S. Wimmer, M. C. Troparevsky, S. N. Khan, S. Mankovsky, H. Ebert, and G. M. Stocks, npj Computational Materials **5**, 1 (2019).

[51]   L. R. Owen, E. J. Pickering, H. Y. Playford, H. J. Stone, M. G. Tucker, and N. G. Jones, Acta Mater. **122**, 11 (2017).

[52]   S. Mu, S. Wimmer, S. Mankovsky, H. Ebert, and G. M. Stocks, Scripta Materialia **170**, 189 (2019).

[53]   S. Ishibashi, Y. Ikeda, F. Körmann, B. Grabowski, and J. Neugebauer, Physical Review Materials **4**, 023608 (2020).

[54]   H. Song, F. Tian, Q.-M. Hu, L. Vitos, Y. Wang, J. Shen, and N. Chen, Physical Review Materials **1**, 023404 (2017).

[55]   Y. Tong, S. Zhao, H. Bei, T. Egami, Y. Zhang, and F. Zhang, in *arXiv e-prints*2019), p. arXiv:1902.09279.

[56]   O. Hellman, P. Steneteg, I. A. Abrikosov, and S. I. Simak, Phys. Rev. B **87**, 104111 (2013).
[57]   O. Hellman, I. A. Abrikosov, and S. I. Simak, Phys. Rev. B **84**, 180301 (2011).
[58]   X. Li, F. Tian, S. Schönecker, J. Zhao, and L. Vitos, Scientific Reports **5**, 12334 (2015).
[59]   B. Feng and M. Widom, Materials Chemistry and Physics **210**, 309 (2018).
[60]   L. J. Santodonato, P. K. Liaw, R. R. Unocic, H. Bei, and J. R. Morris, Nat Commun **9**, 4520 (2018).
[61]   M. C. Troparevsky, J. R. Morris, P. R. C. Kent, A. R. Lupini, and G. M. Stocks, Physical Review X **5**, 011041 (2015).
[62]   F. A. Lindemann, Phys. Z **11**, 609 (1910).
[63]   J. N. Shapiro, Phys. Rev. B **1**, 3982 (1970).
[64]   J. J. Gilvarry, Phys. Rev. **102**, 308 (1956).
[65]   A. Voronel, S. Rabinovich, A. Kisliuk, V. Steinberg, and T. Sverbilova, Phys. Rev. Lett. **60**, 2402 (1988).
[66]   M. Born, The Journal of Chemical Physics **7**, 591 (1939).
[67]   W. Petry, J. Phys. IV France **05**, C2 (1995).
[68]   V. G. Vaks, G. D. Samolyuk, and A. V. Trefilov, Physics Letters A **127**, 37 (1988).
[69]   A. G. Mikhin and Y. N. Osetsky, Journal of Physics: Condensed Matter **5**, 9121 (1993).
[70]   O. El-Atwani *et al.*, Science Advances **5**, eaav2002 (2019).